ORIGINAL PAPER

Differentiation between neurofibromas and malignant peripheral nerve sheath tumors in neurofibromatosis 1 evaluated by MRI

**Akihiko Matsumine · K. Kusuzaki · T. Nakamura · S. Nakazora · R. Niimi ·
T. Matsubara · K. Uchida · T. Murata · I. Kudawara · T. Ueda · N. Naka ·
N. Araki · M. Maeda · A. Uchida**

Abstract

Purpose   The imaging discrimination between neurofibroma (NF) and malignant peripheral nerve sheath tumor (MPNST) is clinically very important. The purpose of this study is to define the criteria for the differential diagnosis between NF and MPNST on MRI in neurofibromatosis 1 (NF1).

Methods   A total of 37 patients with NF1, 18 NFs and 19 MPNSTs were evaluated by MRI at 1.5 T. Magnetic resonance imaging (MRI) findings were compared using univariate and multivariate analyses.

Results   The MRI findings characteristic of MPNST ($p < 0.05$) were an irregular tumor shape (15/19 in MPNST vs. 5/18 in NF), unclear margin (13/19 in MPNST vs. 6/18 in NF), intra-tumoral lobulation (12/19 in MPNST vs. 3/18 in NF), presence of high signal-intensity area on T1-weighted images (T1WI) (12/19 in MPNST vs. 1/18 in NF), no target sign (0/19 in MPNST vs. 12/18 in NF), inhomogeneous enhancement on contract-enhanced T1WI (17/18 in MPNST vs. 9/16 in NF) and a lower rate of enhanced area (54% in MPNST vs. 87% in NF) were critical indicators to differentiate MPNST from NF. A multivariate analysis showed that intra-tumoral lobulation and the presence of a high signal-intensity area on T1WI were considered to be diagnostic indicators of MPNST. The sensitivity and specificity for these two items were 63.2, 83.3, 63.2 and 87.5%, respectively.

Conclusion   MRI shows features which were helpful for differentiating MPNST from NF.

Keywords   Neurofibroma ·
Malignant peripheral nerve sheath tumor ·
Neurofibromatosis 1 · Diagnosis · MRI

A. Matsumine (✉) · K. Kusuzaki · T. Nakamura ·
S. Nakazora · R. Niimi · T. Matsubara · A. Uchida
Department of Orthopaedic Surgery,
Mie University Graduate School of Medicine,
2-174 Edobashi, Tsu, Mie 514-8507, Japan
e-mail: matsumin@clin.medic.mie-u.ac.jp

K. Uchida
Department of Pathology,
Mie University Graduate School of Medicine,
2-174 Edobashi, Tsu, Mie 514-8507, Japan

T. Murata
Department of Pathology, Suzuka General Central Hospital,
1275-53 Yamanohana, Yasuzuka-chyou, Suzuka,
Mie 513-0818, Japan

I. Kudawara · T. Ueda
Department of Orthopaedic Surgery,
National Hospital Organization Osaka National Hospital,
Osaka, 2-1-14 Hotenzaka, Chuo, Osaka 540-0006, Japan

N. Naka · N. Araki
Department of Orthopaedic Surgery,
Osaka Medical Center for Cancer and Cardiovascular Disease,
1-3-3 Nakamichi, Higashinari, Osaka 537-8511, Japan

M. Maeda
Department of Radiology, Mie University School of Medicine,
2-174 Edobashi, Tsu, Mie 514-8507, Japan

Introduction

Neurofibromatosis 1 (NF1) is an autosomal dominant disease, which has characteristic clinical features including café-au-leit spots, skinfold freckling, iris Lisch nodules and neurofibroma (NF) (Fortman et al. 2001; Ramanathan and Thomas 1999; Weisss and Goldbulum 2008; Anonymous 1988; McGaughran et al. 1999). The diagnostic criteria were formulated by the National Institutes of Health

Consensus Development Statement in 1988 (Anonymous 1988).

NF, a benign tumor with typical histological features, occurs in association with NF1. About 5–10% of patients with NF-1 develop malignant peripheral nerve sheath tumors (MPNST) which arise from plexiform neurofibromas (PNF) and often have a poor prognosis (Weisss and Goldbulum 2008; Jee et al. 2004; King et al. 2000; Ramanathan and Thomas 1999; Korf 1999). The tumors sometimes metastasize to the lung, brain, liver, bone soft tissue, regional lymph nodes, skin and retroperitoneum (Lawrence et al. 1987; Weisss and Goldbulum 2008).

There is a critical clinical dilemma in NF1 patients. The histological demarcation between NF with atypical features and a low-grade MPNST is very difficult for the pathologists. In addition, in NF that have undergone malignant transformation, areas of MPNST are commonly located adjacent to areas of NF with a range of atypical features (Weisss and Goldbulum 2008). Furthermore, making an imaging differential diagnosis between NF and MPNST with such complicated features is also difficult. The uncertainty of diagnostic imaging in NF1 patients may therefore lead to multiple operations for neurogenic tumors and a delay in the diagnosis of malignant transformation adversely affect the patients' prognosis (Bhargava et al. 1997; Weisss and Goldbulum 2008). Therefore, the accurate detection of MPNST is very important clinically.

Several investigators have discussed the problems of radiologic diagnosis of MPNST in NF1 patients (Cardona et al. 2003; Levine et al. 1987; Bhargava et al. 1997; Mautner et al. 2003; Solomon et al. 2001; Kumar et al. 1983; Lee et al. 1997; Ferner et al. 2000; Otsuka et al. 2005; Bass et al. 1994; Coleman et al. 1983). Levine et al. (1987) demonstrated that ^{67}Ga scintigraphy appears to be a promising screening technique to identify lesions with malignant degeneration in patients with NF. Previous reports have shown the findings of neurogenic tumors on CT scans to correlate with the histopathological characteristics of the tumors (Kumar et al. 1983; Bass et al. 1994; Coleman et al. 1983). Lee et al. (1997) revealed that SPECT imaging with Ga-67 citrate, Tl-201 chloride and pentavalent Tc-99 m dimercaptosuccinic acid (Tc-99 m(V) DMSA) imaging may be a useful combination for the initial detection of malignant transformation of neurogenic tumors. However, all of these diagnostic modalities have proven to have only limited value for the detection of malignant transformation of neurogenic tumors. The imaging criteria for distinguishing malignant from benign neoplasms are therefore still not clearly defined.

Various radiological techniques have been applied for the detection and follow-up of soft-tissue tumors. Magnetic resonance imaging (MRI) can effectively determine the site and extent of the lesion and its relation to the surrounding structures (Crim et al. 1992; Vanhoenacker et al. 2005; Sakai et al. 1992; Hughes and Spillane 2000). However, the usefulness of MRI in discrimination between NF and MPNST has not yet been determined (Cardona et al. 2003; Bhargava et al. 1997; Mautner et al. 2003). The purpose of this study was to define the criteria of differential diagnosis on MRI between NF and MPNST in NF1 patients.

Patients and methods

Patients and tumors

All of the patients fulfilled the diagnostic criteria of NF1. NF1 was diagnosed according to the National Institutes of Health Criteria (Anonymous 1988). A total of 37 NF-1 patients were enrolled (19 women and 18 men; age 14–80 years: mean age 43 years) with neurogenic tumors in the extremities or on the trunk (Table 1). The patients were collected from three institutes with an orthopedic department specialized in bone and soft-tissue sarcoma (Mie university $n = 30$, National Hospital Organization Osaka National Hospital $n = 5$, Osaka Medical Center for Cancer and Cardiovascular Disease $n = 2$). Regarding the sites of the evaluated tumors, 9 were the upper extremities, 15 the lower extremities, 11 the trunks and 2 in the spine. All of the patients were referred with the preliminary diagnosis of a primary soft-tissue tumor on the basis of their clinical symptoms and radiological examinations, either by Gadolinium-enhanced MRI or contrast-enhanced CT.

Tissue samples were immediately collected from incision biopsied tissue ($n = 5$) or exercised tumor tissue ($n = 32$) and were fixed for 24 h in 10% buffered formalin solution and embedded in paraffin for histological analysis. In all patients, the diagnoses were re-evaluated by the histological examination of the specimens taken at incision biopsy or surgical resection. All of the histological sections were reviewed and categorized by two pathologists (K. U., T. M.). In the case that underwent a tumor excision, the rate of necrotic or hemorrhagic area was microscopically evaluated with the specimens from the maximum cut surface. In the case that underwent an incision biopsy, they were microscopically evaluated using the 4–5 specimens taken from the various portion of the tumor.

An immunohistochemical analysis was performed using the standard methods. MPNST was distinguished from NF by the presence of high cellularity, mitoses and/or geographic area of necrosis (Bhargava et al. 1997; Weisss and Goldbulum 2008). The histological diagnosis was NF in 18 and MPNST in 19. The details of the tumor histology and clinical data of all of the enrolled patients were summarized in Table 1.

Table 1 Details of clinical manifestation, imaging and histological findings

No.	Age	Gender	Diag.	Site	Size (cm)	Depth	Shape	Margin	Lobulation	Cyst	T1WI High signal-intensity area	T2WI Rate of high signal-intensity area	Homogeneity	Target sign	Gd Homogeneity	Enhanced pattern	Rate of enhanced area (%)	Intensity of enhancement	Capsular enhancement	Rate of necrotic area (%)	Rate of hemorrhagic area (%)
1	54	F	MPNST	UE	11	D	I	UC	No	No	Yes	30	Inhomo	No	Inhomo	Irregular	40	Medium	No	<50	10-50
2	57	F	MPNST	LE	4.5	D	R/S	C	No	No	Yes	98	Inhomo	No	Inhomo	Honeycomb	95	Medium	No	>50	10-50
3	61	F	MPNST	LE	15	D	R/S	UC	Yes	Yes	Yes	60	Inhomo	No	Inhomo	Ring	60	Medium	Yes	<50	10-50
4	67	F	NF	T	11	D	F	UC	No	No	No	90	Inhomo	Yes	Inhomo	Ring	70	Strong	Yes	0	1-10
5	29	F	NF	T	4.5	D	R/S	C	No	No	No	90	Inhomo	Yes	Inhomo	Ring	80	Weak	Yes	0	1-10
6	54	F	NF	T	13	S	F	C	No	No	No	95	Inhomo	Yes	Inhomo	Ring	95	Strong	Yes	0	0
7	64	F	NF	S/PS	1	D	R/S	C	No	No	No	100	Homo	No	Homo	Whole	100	Strong	Yes	0	0
8	37	F	NF	T	6	D	I	C	No	No	No	95	Inhomo	Yes	NA	NA	NA	NA	NA	0	0
9	27	M	MPNST	LE	8.5	D	I	UC	Yes	No	No	100	Inhomo	No	Inhomo	Ring	70	Strong	No	<50	1-10
10	56	M	MPNST	LE	8.5	D	I	UC	Yes	No	No	50	Homo	No	Inhomo	Ring	60	Medium	No	<50	1-10
11	39	M	MPNST	UE	14	D	I	UC	Yes	No	Yes	97	Inhomo	No	Inhomo	Ring	50	Strong	Yes	>50	>50
12	18	F	MPNST	LE	6.5	D	I	C	Yes	Yes	No	85	Inhomo	No	Inhomo	Irregular	95	Medium	Yes	<50	0
13	29	M	MPNST	T	13	D	R/S	C	Yes	No	Yes	60	Inhomo	No	NA	NA	NA	NA	NA	>50	>50
14	70	M	MPNST	T	9	D	F	UC	Yes	No	Yes	98	Inhomo	No	Inhomo	Ring	60	Strong	Yes	<50	1-10
15	14	M	NF	LE	6	S	I	UC	No	No	No	95	Inhomo	No	NA	NA	NA	NA	NA	0	0
16	59	M	MPNST	LE	8	D	I	C	Yes	No	No	100	Inhomo	No	Inhomo	Ring	10	Strong	Yes	>50	1-10
17	38	F	MPNST	UE	3	D	I	UC	Yes	No	No	95	Homo	No	Homo	Whole	100	Medium	Yes	0	0
18	68	M	MPNST	LE	12	D	I	UC	Yes	No	Yes	95	Inhomo	No	Inhomo	Ring	50	Strong	Yes	<50	1-10
19	69	F	MPNST	T	17	D	I	UC	Yes	No	Yes	90	Inhomo	No	Inhomo	Ring	30	Strong	Yes	>50	10-50
20	22	M	NF	UE	6	D	R/S	C	No	No	No	98	Inhomo	Yes	Inhomo	Honeycomb	95	Medium	Yes	0	0
21	41	F	MPNST	LE	15	D	I	UC	Yes	No	Yes	98	Inhomo	No	Inhomo	Ring	40	Medium	No	>50	10-50
22	27	F	NF	UE	1.3	D	R/S	C	No	No	No	98	Homo	Yes	Homo	Whole	100	Strong	Yes	0	0
23	61	M	NF	S/PS	1	D	R/S	C	No	Yes	No	70	Inhomo	Yes	Homo	Whole	90	Medium	Yes	0	0
24	18	M	MPNST	T	10	D	I	UC	Yes	Yes	Yes	90	Inhomo	No	Inhomo	Ring	20	Weak	Yes	>50	>50
25	65	M	NF	UE	4.2	D	R/S	C	No	Yes	Yes	90	Inhomo	Yes	Inhomo	Ring	40	Strong	No	<50	1-10
26	29	M	NF	LE	15	D	I	UC	Yes	Yes	No	85	Inhomo	No	Inhomo	Irregular	70	Weak	No	<50	1-10
27	29	F	NF	UE	18	D	R/S	UC	No	No	No	90	Inhomo	Yes	Inhomo	Ring	95	Medium	Yes	0	0
28	25	F	NF	UE	6	S	R/S	UC	No	No	No	95	Inhomo	No	Homo	Whole	98	Strong	Yes	0	0
29	28	M	MPNST	LE	6	D	I	C	No	Yes	No	95	Inhomo	No	Inhomo	Ring	70	Medium	Yes	<50	0
30	20	F	NF	LE	9	D	I	C	Yes	Yes	No	95	Inhomo	Yes	Homo	Whole	80	Medium	Yes	<50	1-10
31	80	F	MPNST	LE	2	D	I	C	No	No	No	100	Homo	No	Inhomo	Ring	10	Weak	Yes	<50	0
32	24	F	NF	UE	2.5	D	R/S	C	No	No	No	70	Inhomo	Yes	Homo	Whole	96	Strong	Yes	0	0
33	36	M	NF	LE	6.3	D	R/S	C	No	No	No	95	Inhomo	No	Inhomo	Irregular	80	Weak	Yes	0	0
34	34	M	NF	LE	9	D	F	C	No	No	No	95	Inhomo	No	Homo	Whole	100	Weak	Yes	0	0

Table 1 continued

No.	Age	Gender	Diag.	Site	Size (cm)	Depth	Shape	Margin	Lobulation	Cyst	T1WI High signal-intensity area	T2WI Rate of high signal-intensity area	T2WI Homogenesity	T2WI Target sign	Gd Homogenesity	Gd Enhanced pattern	Gd Rate of enhanced area (%)	Gd Intensity of enhancement	Gd Capsular enhancement	Rate of necrotic area (%)	Rate of hemorrhagic area (%)
35	62	F	NF	T	4.5	D	I	UC	Yes	No	No	90	Inhomo	Yes	Inhomo	Ring	95	Medium	Yes	0	0
36	44	M	MPNST	T	10	D	I	UC	Yes	Yes	Yes	95	Inhomo	No	Inhomo	Ring	50	Strong	Yes	<50	1–10
37	32	M	MPNST	T	6	D	I	UC	No	Yes	Yes	40	Inhomo	No	Inhomo	Ring	50	Medium	Yes	>50	1–10

F female, *M* male, *diag.* diagnosis, *MPNST* malignant peripheral nerve sheath tumor, *NF* neurofibroma, *UE* upper extremity, *LE* lower extremity, *T* trunk, *S/PS* spine/para-spine, *D* deep, *S* superficial, *I* irregular, *R/S* round/spindle, *F* flat, *UC* unclear, *C* clear, *T1WI* T1-weighted imaging, *T2WI* T2-weighted imaging, *NA* not available, *inhomo* inhomogeneous, *homo* homogeneous

MRI and imaging data analysis

All images were obtained using a surface coil. The studies were conducted within the guidelines of the research committees of this institution. Informed consent was obtained from patients or their authorized guardians. MRI studies were performed using 1.5-T MR units (Signa, GE Medical Systems, Milwaukee, WI, USA: $n = 30$ and Magnetom H15 1.5T, Siemens, Munich, Germany: $n = 7$). MRI sequences included T1-weighted imaging (T1WI) (TR/TE = 500 ms/ 9 ms, matrix size = 256×192, excitations = 2), fast spin echo T2WI with or without fat suppression (TR/ TE = 3,000 ms/90 ms, matrix size = 256×192, echo train length = 8, excitations = 2) and contrast-enhanced T1WI with or without fat suppression. MRIs were retrospectively reviewed by an experienced musculoskeletal radiologist who was unaware of the surgical results (MM), for the presence or absence of individual imaging criteria. On all imaging sequences, the tumors were categorized as homogeneous or heterogeneous and as low signal-intensity, intermediate signal-intensity or high signal-intensity relative to skeletal muscle on T1WI and T2WI.

The tumor characteristics including tumor size, location, tumor shape, appearance of margin, lobulation, signal-intensity of T1WI, rate of high signal-intensity area in T2WI, homogeneity on T2WI, target sign, homogeneity on gadolinium-enhanced images, an enhanced pattern, the rate of the gadolinium-enhanced area, the intensity of gadolinium-enhancement, capsular enhancement and cyst formation were evaluated. Tumor size was defined by measuring the maximum major axis on T2WI. Tumor depth was defined by evaluating the relationship between tumor and superficial fascia. The tumor locations were categorized into four groups; upper extremities, lower extremities, spine/paraspine and trunk. Tumor shape could be categorized into three groups; namely, an irregular, round/spindle and flat shape on T2WI. The characteristics of the tumor margin were categorized on T2WI into two groups; clear and unclear. "Unclear" was defined when the tumor had infiltrated to the surrounding structures. The lobulation was defined on T1WI and T2WI when tumor was separated by fibrous septum forming a tumor nodule. The presence of a high signal-intensity area was determined on T1WI. The rate of high signal-intensity area on T2WI was calculated using image analysis system (IBM Clinical Information System-Image, IBM Japan, Tokyo). Homogeneity on T2WI, presence of target sign on T2WI and homogeneity on gadolinium-enhanced images were also determined. Target sign was defined as a hyperintense rim with centrally decreased intensity to muscle on T2-weighted sequences (Bhargava et al. 1997). The enhanced patterns were categorized into four patterns: ring pattern, whole pattern, irregular pattern and

Table 2 Relationship between the imaging findings and histological diagnosis

Clinical manifestation	MPNST	NF	p value
Gender			
Male	11	7	0.2476[a]
Female	8	11	
Age	38.8	46.7	0.1812[b]
Tumor size			
Mean (cm)	9.4	6.9	0.0674[b]
Depth			
Deep	19	16	0.2297[c]
Superficial	0	2	
Location			
Upper extremities	6	3	0.1923[a]
Lower extremities	5	10	
Spine/Parapsine	2	0	
Trunk	5	6	
Shape			
Irregular	15	5	0.0201[a]
Round/spindle	3	10	
Flat	1	3	
Margin			
Clear	6	12	0.0328[a]
Unclear	13	6	
Lobulation			
Lobulated	12	3	0.0069[c]
Unlobulated	7	15	
High signal-intensity area on T1-weighted images			
Yes	12	1	0.004[c]
No	7	17	
Rate of high signal-intensity area on T2-weighted images			
Mean	82.9	90.9	0.9014[b]
Homogenesity on T2-weighted images			
Homogeneous	2	1	>0.9999[c]
Inhomogeneous	17	17	
Target sign			
Yes	0	12	<0.0001[c]
No	19	6	
Homogenesity on CE -T1-weighted images			
Homogeneous	1	7	0.0145[c]
Inhomogeneous	17	9	
Enhanced pattern			
Ring	14	6	0.0548[a]
Whole	1	7	
Irregular	2	2	
Honeycomb	1	1	
Rate of enhanced area (%)			
Mean	53.75	86.5	0.0006[b]

Table 2 continued

Clinical manifestation	MPNST	NF	p value
Intensity of enhancement			
Strong	7	7	0.4279[a]
Middle	9	5	
Weak	2	4	
Capsular enhancement			
Yes	13	14	0.4054[c]
No	5	2	
Cyst formation			
Yes	4	3	>0.9999[c]
No	15	15	

[a] χ^2 test for independence

[b] Mann–Whitney's Test

[c] Fisher's exact probability test

honeycomb pattern. The signal intensity of each lesion after contrast enhancement was calculated in terms of mean pixel values in a computer-drawn region of interest. The region of interest was drawn to encompass the maximum region of enhancement for each lesion as determined on post-contrast images. Thereafter, the signal intensity could be classified into three categories: strong, middle, and weak. The intensity of gadolinium-enhancement was classified into three categories; strong, middle and weak. The rate of enhanced area after gadolinium administration was calculated on T1WI using image analysis system (IBM Clinical Information System-Image, IBM). The presence of capsular enhancement was determined when either the capsule or the pseudo capsule was enhanced after gadolinium administration. The presence of intra-tumoral cyst formation was determined when the rounded area was demonstrated as low to iso signal-intensity area on T1WI and as very high signal-intensity area on T2WI without any enhancement after gadolinium administration.

Statistical analysis

For the univariate analysis, the chi-square test for independence was used to detect significant differences in the characteristics between NF and MPNST. When the number of expectation values was less than 5, Fisher's exact probability test was used. If a variable was continuous variants such as age, tumor size, the Mann–Whitney's test was employed. For the multivariate analysis of variables which might be useful to distinguish between NF and MPNST, a logistic regression analysis was used.
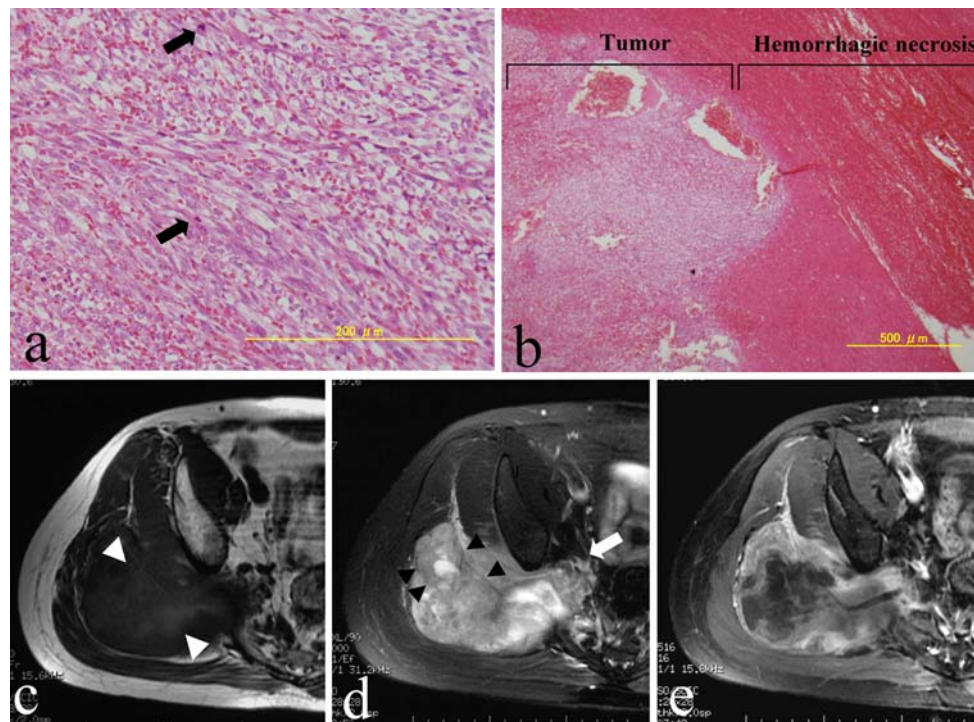
Fig. 1 Microscopic findings and MRI of a 44-years-old male (no. 36) with typical MPNST are demonstrated. **a** Microscopic findings showed proliferation of spindle cells with nuclear pleomorphism and mitosis (*closed arrow*). **b** About 40% of the area of the cross-section showed massive necrosis with hemorrhage. **c–e** MRI showed the following indicators to differentiate MPNST from NF: an irregular tumor shape, unclear margin (*open arrow*), presence of intra-tumoral lobulation (*closed triangle*), presence of high signal-intensity area on T1-weighted images (*open triangle*), no target sign, nohomogeneous enhancement on contract-enhanced T1-weighted images and a lower rate of enhanced area (**c** T1-weighted spin-echo image, TR500/TE8, **d** fat-suppressed T2-weighted spin-echo image, TR4000/TE81, **e** fat-suppressed gadolinium-enhanced T1- weighted spin-echo image, TR516/TE16)

When the relationship between the rate of gadolinium-enhanced area or the presence of high signal-intensity area and the microscopic findings in the surgical specimens was assessed, Spearman's rank correlation was employed. A p value less than 0.05 was considered to indicate a statistically significant difference. All these univariate and multivariate analyses were performed using the StatView statistical software program (version 5.0; SAS Institute Inc. Cary, North Carolina).

Results

First, all MRI of the neurogenic tumors of 37 NF1 patients were examined and the following imaging characteristics were assessed: including the tumor size, tumor location, tumor shape, appearance of tumor margin, presence of intratumoral lobulation, signal-intensity on T1WI, rate of high signal-intensity area on T2WI, homogeneity on T2WI, target sign, homogeneity on gadolinium-enhanced images, an enhanced pattern, rate of gadolinium-enhanced area, intensity of enhancement, capsular enhancement and cyst formation. Next, a pathologist (K. U., T. M.) re-examined

all specimens and re-evaluated the histological diagnosis. There were no discrepancies between the initial histological diagnosis and the re-evaluated diagnosis (Table 1). Then the relationships between the MRI findings and histological diagnosis we analyzed (Table 2).

There were significant differences ($p \leq 0.05$) between MPNST and NF in the following MRI findings: an irregular tumor shape (79% [15/19] in MPNST vs. 28% [5/18] in NF), unclear margin (68% [13/19] in MPNST vs. 33%[6/18] in NF), intra-tumoral lobulation (63% [12/19] in MPNST vs. 17% [3/18] in NF), presence of high signal-intensity area on T1WI (63% [12/19] in MPNST vs. 6% [1/18] in NF), no target sign (0% [0/19] in MPNST vs. 67% [12/18] in NF), inhomogeneous enhancement on contract-enhanced T1WI (94% [17/18] in MPNST vs. 56% [9/16] in NF) and a lower rate of enhanced area (54% in MPNST vs. 87% in NF), and these MRI findings were significant indicators to differentiate MPNST from NP (Fig. 1).

Analysis of gender, age, tumor size, depth, location, rate of high signal-intensity area on T2WI, homogeneity on T2WI, an enhanced pattern, intensity of enhancement, capsular enhancement and cyst formation did not show any significant association with the presence or absence of malignancy.
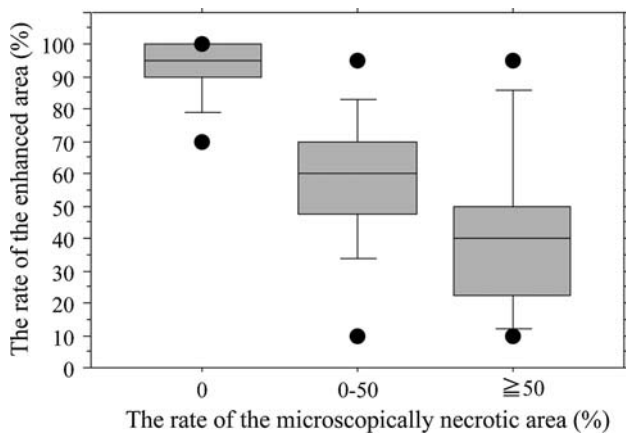
Fig. 2 The relationship between the rate of the enhanced area (%) on gadolinium-enhanced T1-weighted images and the rate of the microscopically necrotic area (%). The rate of the gadolinium-enhanced area on T1-weighted images showed a significant negative correlation to the rate of microscopic necrotic area (Spearman's rank correlation: $p < 0.0001$)

To confirm the reliability of the interpretation of MRI, the relationship between the rate of gadolinium-enhanced area and the rate of microscopic necrotic area were assessed in the surgical specimens. The rate of the gadolinium-enhanced area on T1WI showed significant negative correlation to the rate of microscopic necrotic area (Spearman's rank correlation: $p < 0.0001$) (Fig. 2). These results indicate that gadolinium-enhanced MRI correctly reflected the extent of microscopic necrosis.

Next, a multivariate analysis was performed to examine the independent factors useful for differential diagnosis between NF and MPNST. A logistic regression analysis was employed. Thereafter, the presence of intratumoral lobulation and the presence of high signal-intensity area on T1WI were found to be diagnostic characteristic of MPNST in order to differentiate it from NF (Table 3). The sensitivity and specificity for these two items were 63.2% (12/19), 83.3% (15/18), 63.2% (12/19) and 87.5% (7/8), respectively.

Finally, to confirm the cause of the presence of the high intensity area on T1WI in MPNST, the histological specimens we examined in detail and the relationship between the presence of a high signal-intensity area on MRI and rate of hemorrhagic area were assessed in the specimens. As a result, the presence of high intensity area was correctly related to the rate of hemorrhagic area (Spearman's rank correlation: $p < 0.0001$) (Fig. 3). This result suggests that a high signal-intensity area on MRI thus reflects the presence of intratumoral hemorrhaging.

Discussion

NF in NF1 patients involving major nerves should be treated conservatively because a complete tumor resection may lead to a major neurological deficit which thus disrupts the patient's routine. About 5–10% of patients with NF1 develop MPNST which forms plexiform NF and often leads to a poor prognosis (Weisss and Goldbulum 2008; Anonymous 1988; Jee et al. 2004; King et al. 2000; Ramanathan and Thomas 1999; Korf 1999). Therefore, it is extremely important to accurately detect the malignant transformation as soon as possible in NF1 patients. This malignant transformation is suspected when clinical features such as pain, increasing of tumor size and development of neurological symptoms occur (King et al. 2000; Ramanathan and Thomas 1999; Korf 1999; Weisss and Goldbulum 2008), but these findings can also be observed in benign lesions (Ferner et al. 2000; Weisss et al. 2008).

There are some limited reports which have previously attempted to differentiate MPNST from benign lesions by MRI. Levine et al. indicated that MRI could not generally distinguish malignant from benign lesions after an examination of symptomatic neoplasm (three benign and five malignant) (Levine et al. 1987). However, this study has some limitations in regard to the fact that gadolinium-contrast enhancement was not performed. In a small cohort study, Mautner et al. (2003) indicated that the development of the malignant tumors was detected because of imaging changes, with inhomogeneous contrast enhancement. However, there are still no generally accepted imaging criteria for distinguishing malignant from benign neoplasms in the neurogenic tumors of NF1 patients.

The present series showed that an irregular tumor shape, unclear margin, presence of intra-tumoral lobulation, presence of high signal-intensity area on T1WI, no target sign, inhomogeneous enhancement on contract-enhanced T1WI and a lower rate of enhanced area were critical indicators to differentiate MPNST from NF. These results indicate that a careful examination of MRI may be able to reduce performance of unnecessary surgery in NF1 patients.

An irregular tumor shape was more frequently observed in MPNST than in NF (15/19 in MPNST vs. 5/18 in NF). An irregular tumor shape is one of the most critical

Table 3 Results of a logistic regression analysis of factors which predict MPNST in NF1 patients on MRI

Variable	OR	95% CI	p value
Lobulation			
NF	1	1.2–48.0	0.031
MPNST	2		
High signal-intensity area on T1-weighted images			
NF	1	2.5–277.5	0.006
MPNST	3.3		

OR Odds ratio, *NF* neurofibroma, *MPNST* malignant peripheral nerve sheath tumor, *NF1* neurofibromatosis 1
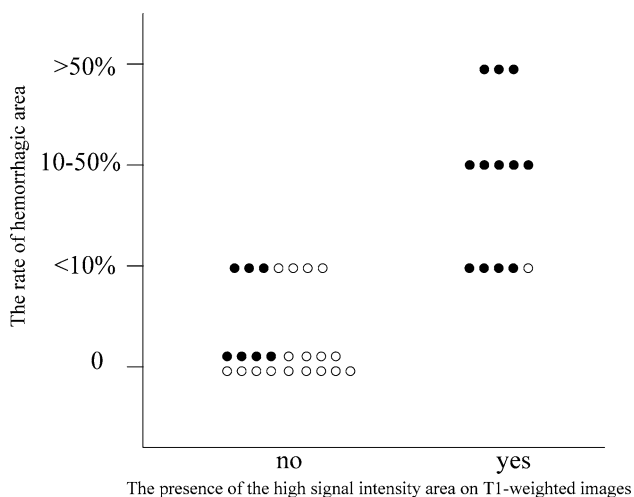
Fig. 3 The relationship between the presence of a high signal-intensity area on MRI and the rate of hemorrhagic area. The presence of a high intensity area was closely related to the rate of hemorrhagic area (Spearman's rank correlation $p \leq 0.0001$). *Open circle*, neurofibroma; *closed circle*, malignant peripheral nerve sheath tumor

characteristics suggestive of malignant soft-tissue tumors (Crim et al. 1992; Kransdorf et al. 1989). Crim et al. (1992) evaluated the ability to distinguish benign from malignant soft-tissue masses with MRI and demonstrated that most malignant masses have irregular or partially irregular margins. Irregular shape in malignancy is resulting from the unsynchronized cell growth with invasive characteristics.

An unclear margin was also more common characteristic in MPNST than in NF (13/19 in MPNST vs. 6/18 in NF), which was consistent with a previous report (Levine et al. 1987). An unclear margin may be due to infiltration of the tumor to the surrounding tissue.

The intra-tumoral lobulation that was observed in 12 of 19 MPNST and 3 of 18 NF is considered to be the result of a network-like growth of NF involving multiple fascicles of a nerve and multiple branches of a large nerve, leading to a diffuse mass of thickened nerves (Korf 1999). Intra-tumoral lobulation is one of the characteristics of PNF (Korf 1999; Weisss and Goldbulum 2008). King et al. (2000) indicated that 64% of MPNST occurred in the patients with a previous history of preexisting PNF. This suggests that MPNST retains the similar histological architecture which can be detectable by MRI, thus reflecting the origin of MPNST.

The presence of high signal-intensity area on T1WI (12/19 in MPNST vs. 1/18 in NF) was also critical indicator to diagnose MPNST. On T1WI of MRI, a high intensity area usually means the presence of fat tissue or a hemorrhagic area, although MR findings of a hemorrhagic area depends on methemoglobin, hemosiderin, oxyhemoglobin, deoxyhemoglobin (Vanhoenacker et al. 2005). To confirm the cause of the presence of a high intensity area on T1WI in

MPNST, the histological specimens we examined in detail and this demonstrated that the presence of a high intensity area was correctly related to the rate of hemorrhagic area. Therefore, a high intensity area on MRI indicates an intratumoral hemorrhage which is a property of malignancy.

A target sign on T2WI with a rim of high signal peripherally and low signal centrally is characteristic sign of a neurogenic tumor (Weisss and Goldbulum 2008). Previous studies indicate that a target sign on T2WI corresponds pathologically to central fibrocollagenous tissue and peripheral predominantly myxoid tissue (Sakai et al. 1992). In the present study, target sign was observed in 0/19 (0%) of MPNST and in 12/18 (67%) of NF, which was consistent with a previous study indicating that a target sign was seen in all 12 NF and 1 of the 11 MPNST (Bhargava et al. 1997). Namely, no target sign on T2WI is helpful in differentiating MPNST from NF.

MPNST in patients with NF1 frequently showed inhomogeneous enhancement on contract-enhanced T1WI (17/18 in MPNST vs. 9/16 in NF), which was consistent with a previous study (Mautner et al. 2003). This lack of homogeneity is due to necrosis and hemorrhage as shown on microscopic examinations. The development of the malignant tumors can be detected because of imaging changes, inhomogeneous contrast enhancement.

MRI following the administration of intravenous contrast materials improves contrast resolution in evaluation of soft-tissue tumors (Benedikt et al. 1994). Imaging following contrast is particularly important with masses that have high water content (cyst vs. myxoid neoplasm) or are composed of prominent necrotic/hemorrhagic foci allowing identification and differentiation of these regions from enhancing solid cellular tissue (van der Woude et al. 1998). The rate of an enhanced area in MPNST was statistically lower than in NF (54% in MPNST vs. 87% in NF). Moreover, the rate of a gadolinium-enhanced area on T1-images showed significant negative correlation to the rate of microscopic necrotic area as shown in the previous CT-based study (Coleman et al. 1983). This result indicates that gadolinium-enhanced MRI correctly reflected the extent of microscopic intratumoral necrosis in neurogenic tumor of NF1 patients.

In the present study, a multivariate analysis showed that intra-tumoral lobulation and the presence of a high intensity area on T1WI were differential diagnostic characteristics of MPNST from NF. Therefore, the sensitivity and specificity were calculated. The sensitivity and specificity of intratumoral lobulation were 63.2% (12/19) and 83.3% (15/18), respectively. The sensitivity and specificity of the presence of high intensity area on T1WI were 63.2% (12/19) and 87.5% (7/8), respectively. These results suggest that the MRI findings were helpful for differentiating MPNST from NF in NF1 patients. However,

no single finding or group of findings allowed the definitive diagnosis of either.

The limitations of this study include that the reviewers of the MRI were aware that all patients had a pathologically confirmed MPNST or NF, which may have increased the sensitivity for detecting each of the MRI findings. Therefore, further investigation is needed.

In conclusion, the goal of this study was to define the criteria of differential diagnosis between NF and MPNST on MRI in NF1 patients. MRI findings suggestive of MPNST were: an irregular tumor shape, unclear margin, intra-tumoral lobulation, presence of high signal-intensity area on T1WI, no target sign, inhomogeneous enhancement on contract-enhanced T1WI and a lower rate of enhanced area. Since NF with atypical features may undergo malignant transformation to a MPNST, careful interpretation of MRI regarding these imaging characteristics suggesting malignant transformation are therefore recommended, to avoid any unnecessary surgical intervention. MRI showed features helpful for differentiating MPNST from NF, although no single findings or combination of findings allowed absolute differentiation. To the best of our knowledge, this is the first report to define the imaging criteria of MPNST on MRI in NF1 patients.

References

Bass JC, Korobkin M, Francis IR, Ellis JH, Cohan RH (1994) Retroperitoneal plexiform neurofibromas: CT findings. AJR Am J Roentgenol 163:617–620

Benedikt RA, Jelinek JS, Kransdorf MJ, Moser RP, Berrey BH (1994) MR imaging of soft-tissue masses: role of gadopentetate dimeglumine. J Magn Reson Imaging 4:485–490. doi:10.1002/jmri.1880040341

Bhargava R, Parham DM, Lasater OE, Chari RS, Chen G, Fletcher BD (1997) MR imaging differentiation of benign and malignant peripheral nerve sheath tumors: use of the target sign. Pediatr Radiol 27:124–129. doi:10.1007/s002470050082

Cardona S, Schwarzbach M, Hinz U, Dimitrakopoulou-Strauss A, Attigah N, Mechtersheimer section sign G, Lehnert T (2003) Evaluation of F18-deoxyglucose positron emission tomography (FDG-PET) to assess the nature of neurogenic tumours. Eur J Surg Oncol 29:536–541. doi:10.1016/S0748-7983(03)00055-6

Coleman BG, Arger PH, Dalinka MK, Obringer AC, Raney BR, Meadows AT (1983) CT of sarcomatous degeneration in neurofibromatosis. AJR Am J Roentgenol 140:383–387

Crim JR, Seeger LL, Yao L, Chandnani V, Eckardt JJ (1992) Diagnosis of soft-tissue masses with MR imaging: can benign masses be differentiated from malignant ones? Radiology 185:581–586

Ferner RE, Lucas JD, O'Doherty MJ, Hughes RA, Smith MA, Cronin BF, Bingham J (2000) Evaluation of (18)fluorodeoxyglucose positron emission tomography ((18)FDG PET) in the detection of malignant peripheral nerve sheath tumours arising from within plexiform neurofibromas in neurofibromatosis 1. J Neurol Neurosurg Psychiatry 68:353–357. doi:10.1136/jnnp.68.3.353

Fortman BJ, Kuszyk BS, Urban BA, Fishman EK (2001) Neurofibromatosis type 1: a diagnostic mimicker at CT. Radiographics 21:601–612

Hughes TM, Spillane AJ (2000) Imaging of soft tissue tumours. Br J Surg 87:259–260. doi:10.1046/j.1365-2168.2000.01412.x

Jee WH, Oh SN, McCauley T, Ryu KN, Suh JS, Lee JH, Park JM, Chun KA, Sung MS, Kim K, Lee YS, Kang YK, Ok IY, Kim JM (2004) Extraaxial neurofibromas versus neurilemmomas: discrimination with MRI. AJR Am J Roentgenol 183:629–633

King AA, DeBaun MR, Riccardi VM, Gutmann DH (2000) Malignant peripheral nerve sheath tumors in neurofibromatosis 1. Am J Med Genet 93:388–392. doi:10.1002/1096-8628(20000828)93:5<388::AID-AJMG8>3.0.CO;2-#

Korf BR (1999) Plexiform neurofibromas. Am J Med Genet 89: 31–37. doi:10.1002/(SICI)1096-8628(19990326)89:1<31::AID-AJMG7>3.0.CO;2-W

Kransdorf MJ, Jelinek JS, Moser RP Jr, Utz JA, Brower AC, Hudson TM, Berrey BH (1989) Soft-tissue masses: diagnosis using MR imaging. AJR Am J Roentgenol 153:541–547

Kumar AJ, Kuhajda FP, Martinez CR, Fishman EK, Jezic DV, Siegelman SS (1983) Computed tomography of extracranial nerve sheath tumors with pathological correlation. J Comput Assist Tomogr 7:857–865

Lawrence W Jr, Donegan WL, Natarajan N, Mettlin C, Beart R, Winchester D (1987) Adult soft tissue sarcomas. A pattern of care survey of the American College of Surgeons. Ann Surg Apr 205:349–359

Lee J, Sohn SK, Ahn BC, Chun KA, Lee K, Kim CK (1997) Sarcomatous transformation of neurofibromas. Comparative imaging with Ga-67, Tl-201, Tc-99 m pentavalent DMSA and Tc-99 m MIBI. Clin Nucl Med 22:610–614. doi:10.1097/00003072-199709000-00006

Levine E, Huntrakoon M, Wetzel LH (1987) Malignant nerve-sheath neoplasms in neurofibromatosis: distinction from benign tumors by using imaging techniques. AJR Am J Roentgenol 149:1059–1064

Mautner VF, Friedrich RE, von Deimling A, Hagel C, Korf B, Knöfel MT, Wenzel R, Fünsterer C (2003) Malignant peripheral nerve sheath tumours in neurofibromatosis type 1: MRI supports the diagnosis of malignant plexiform neurofibroma. Neuroradiology 45:618–625. doi:10.1007/s00234-003-0964-6

McGaughran JM, Harris DI, Donnai D, Teare D, MacLeod R, Westerbeek R, Kingston H, Super M, Harris R, Evans DG (1999) A clinical study of type 1 neurofibromatosis in north west England. J Med Genet 36:197–203

Anonymous (1988) Neurofibromatosis. Conference statement. National Institutes of Health Consensus Development Conference. Arch Neurol 45:575–578

Otsuka H, Graham MM, Kubo A, Nishitani H (2005) FDG-PET/CT findings of sarcomatous transformation in neurofibromatosis: a case report. Ann Nucl Med 19:55–58

Ramanathan RC, Thomas JM (1999) Malignant peripheral nerve sheath tumours associated with von Recklinghausen's neurofibromatosis. Eur J Surg Oncol 25:190–193. doi:10.1053/ejso.1998.0625

Sakai F, Sone S, Kiyono K, Maruyama A, Ueda H, Aoki J, Kawai T, Ishii K, Morimoto M, Haniuda M et al (1992) Intrathoracic neurogenic tumors: MR-pathologic correlation. AJR Am J Roentgenol 159:279–283

Solomon SB, Semih Dogan A, Nicol TL, Campbell JN, Pomper MG (2001) Positron emission tomography in the detection and management of sarcomatous transformation in neurofibromatosis. Clin Nucl Med 26:525–528. doi:10.1097/00003072-200106000-00009

van der Woude HJ, Verstraete KL, Hogendoorn PC, Taminiau AH, Hermans J, Bloem JL (1998) Musculoskeletal tumors: does fast dynamic contrast-enhanced subtraction MR imaging contribute to the characterization? Radiology 208:821–828

Vanhoenacker FM, De Schepper AM, Gielen JL, Parizel PM (2005) MR imaging in the diagnosis and management of inheritable musculoskeletal disorders. Clin Radiol 60:160–170. doi: 10.1016/j.crad.2004.06.003

Weisss SW, Goldbulum JR (2008) Malignant tumors of the perioheral nerves. In: Weisss SW, Goldbulum JR (eds) Enzinger and Weiss's soft tissue tumors, 5th edn. Elsevier, Netherlands, pp 903–944